The Trans Effect in Square-Planar Platinum(II) Complexes—A Density Functional Study

ZDENEK CHVAL,[1] MIROSLAV SIP,[1] JAROSLAV V. BURDA[2]
[1]*Department of Biophysics, Faculty of Health and Social Studies, University of South Bohemia, J. Boreckeho 27, 370 11 Ceske Budejovice, Czech Republic*
[2]*Department of Chemical Physics and Optics, Faculty of Mathematics and Physics, Charles University, Ke Karlovu 3, 121 16 Prague 2, Czech Republic*

Received 25 October 2007; Revised 12 February 2008; Accepted 17 February 2008
DOI 10.1002/jcc.20980
Published online 28 April 2008 in Wiley InterScience (www.interscience.wiley.com).

Abstract: The mechanism of substitution water exchange reactions in square planar trans-Pt[$(NH_3)_2T(H_2O)]^{n+}$ complexes is studied (T=H_2O, NH_3, OH^-, F^-, Cl^-, Br^-, H_2S, CH_3S^-, SCN^-, CN^-, PH_3, CO, CH_3^-, H^-, C_2H_4). The trans effect is explained in terms of σ-donation and π-back-donation whose relative strengths are quantified by the changes of electron occupations of 5d platinum atomic orbitals. The σ-donation strength is linearly correlated with the Pt—H_2O (leaving ligand) bond length (trans influence). The kinetic trans effect strength correlates proportionally with the σ-donation ability of the trans-ligand except the ligands with strong π-back-donation ability that stabilizes transition state structure. The σ-donation ability of the ligand is dependent on the σ-donation strength of the ligand in the trans position. Therefore the trans effect caused by σ-donation can be understood as a competition between the trans-ligands for the opportunity to donate electron density to the central Pt(II) atom. The influence of the trans effect on the reaction mechanism is also shown. For ligands with a very strong σ-donation (e.g. CH_3^- and H^-), the substitution proceeds by a dissociative interchange (I_d) mechanism. Ligands with strong π-back donation ability (e.g. C_2H_4) stabilize the pentacoordinated intermediate and the substitution proceeds by a two step associative mechanism. For ligands with weak σ-donation and π-back-donation abilities, the highest activation barriers have to be overcome and substitutions can be described by an associative interchange (I_a) mechanism. The results are supported by the energy decomposition and the natural orbital analysis.

 J Comput Chem 29: 2370–2381, 2008

Key words: trans effect; reaction mechanism; square planar platinum(II) complexes; σ-donation; π-back-donation

Introduction

The ligand substitution reactions in square-planar Pt(II) complexes comprise a very intensively investigated class of processes. The trans effect was already observed by Chernyaev in the twenties of the last century.[1] Since then the kinetics of many other systems has been explained by the trans effect.[2] By the trans effect is meant the labilization of a ligand in trans position to certain other ligand. For platinum complexes there is a number of experimental studies available comparing trans effects of different ligands.[3] The intensity of the trans effect (as measured by the increase in the rate of substitution of the trans ligand) follows this sequence:

$$F^-, H_2O, OH^- < NH_3 < py < Cl^- < Br^- < I^-, SCN^-, NO_2^-$$
$$SC(NH_2)_2, Ph^- < SO_3^{2-} < PR_3, AsR_3, SR_2, CH_3^- < H^-,$$
$$NO, CO, CN^-, C_2H_4$$

Since the trans effect is a kinetic phenomenon, its origin lies in reactant destabilization and/or in the transition state stabilization. The first effect is usually expressed by the Pt- trans ligand bond elongation and it is sometimes called as the trans influence.

The finding of the anticancer activity of cisplatin (cis-diamminedichloroplatinum(II)) and its derivatives further enhanced the interest of this class of compounds.[4] Cisplatin is one of the best theoretically described systems.[5–14] The mode of

Additional Supporting Information may be found in the online version of this article.

Correspondence to: Z. Chval; e-mail: chval@jcu.cz or J.V. Burda; e-mail: burda@karlov.mff.cuni.cz

Contract/grant sponsors: COST and Ministry of Education of the Czech Republic; contract/grant number: D20.005

Contract/grant sponsor: GA-AV; contract/grant number: IAA400550701

Contract/grant sponsor: MSM; contract/grant number: 0021620835

action of cisplatin includes hydrolysis in the first step followed by the binding to the guanine N7 atom of DNA. Both these steps were described theoretically in number of studies during recent years.[6,9,14–22] In the hydrolysis step the chloride ligand is replaced by a water ligand which is exchanged by the guanine in the next step. Both substitution reactions have a similar one-step mechanism and go via pentacoordinated transition states.[6,15] The NH_3 group with a weak trans effect inheres in the *trans* position with respect to these substitutions. A thorough study of substitution reactions in the square planar $Pt[(NH_3)_x(H_2O)_yCl_z]^{+2-z}$ ($x + y + z = 4$) complexes was done by Cooper and Ziegler.[23] Since all ligands considered in the cited study have a weak trans effect strengths, all possible substitution reactions were described by a facilitated dissociative mechanism (or an associative interchange (I_a) mechanism as it is denoted in this contribution) overcoming one pentacoordinated transition state.

Trans effect of biologically active ligands was studied by Lau and Deubel.[24] The kinetic trans effect of the biomolecules significantly differs from the thermodynamic trans influence. The sulfur ligands show a larger trans effect than nitrogen ligands and water.

In the theoretical paper dealing with boryl ligands,[25] i.e. ligands with very strong trans influence, results were analyzed by the natural orbital analysis. A good correlation between the trans influence strength and the percentage contribution of Pt in Pt—B σ bond was found. These properties are also correlated with the ratio of the boron p- to s-orbital population in the Pt—B σ bond. Very recently trans- influence of boryl ligands was also studied experimentally by Braunschweig et al.[26]

In this contribution we show how the ligands with different trans effect strengths influence not only the value of activation energy (i.e. kinetics) of substitution reactions but also the reaction mechanism itself. We use similar systems as were used in the pioneer study of Lin and Hall.[27] However this time electron correlation is included, all the stationary points including transition states are fully optimized and influence of much larger number of ligands in the trans position is compared. Moreover theoretical methods for the analysis of the nature of bonding interactions (such as the natural bond orbital analysis and the energy decomposition analysis) are currently available. Thus we are able to show details about the substitution reactions that could not be revealed in the cited study.

Computational Details

The calculations were performed with the Gaussian 03 (G03) program package.[28] All geometries were fully optimized using B3LYP functional.[29] LANL2DZ valence basis set with an extra set of f functions of exponent 0.78 and relativistic effective core potentials (ECP's) were used for the platinum atom. Pt is treated as an 18-electron system with both $n = 5$ and $n = 6$ shells considered as valence electron shells. This basis set on the Pt atom is designated as LANL2DZ*. For the main group elements the split valence 6-31G* basis set was used. These calculations are designated as B3LYP/BSI in the further text. Selected structures were optimized by a substantially improved MWB-60(2f)/6-311++G(2d,2p) basis set. It means platinum atom was treated using Dresden-Stuttgart pseudopotentials.[30] The suggested basis set was extended with two extra sets of f functions with exponents of 1.4193 and 0.4662.[10] The main group elements are described by 6-311++G(2d,2p) basis set. These calculations are designated as B3LYP/BSII in the further text.

The nature of the obtained stationary points was always checked by a vibrational analysis. Thermal contributions to the energetic properties were calculated using microcanonical ensemble of statistical mechanics at standard conditions ($T = 298$ K, $p = 101.325$ kPa). Single point energy evaluations on the optimized geometries were carried out with a more flexible MWB-60(2fg)/6-311++G(2df,2dp) basis set. Platinum basis set was augmented by an extra set of g functions with the exponent 1.2077.

To evaluate the solvent influence on the energetics of the reaction, single point calculations on the gas phase optimized geometries were performed using CPCM continuum solvation model on the B3LYP/MWB-60(2fg)/6-311++G(2df,2dp) level of theory (the same level as the gas-phase single points). All solvation calculations were carried out in water ($\varepsilon = 78.39$). Default CPCM parameterization as implemented in G03 was used.

Atomic charges were derived by Weinhold's natural population analysis (NPA) using the natural bond orbital (NBO) partitioning scheme.[31,32]

In this study we deal with substitution reactions *trans*-$Pt[(NH_3)_2(H_2O)T]^{n+}$ + $H_2O \leftrightarrow$ *trans*-$Pt[(NH_3)_2(H_2O)T]^{n+}$ + H_2O. Water ligand that is in the trans position with respect to the T ligand (T=H_2O, NH_3, OH^-, F^-, Cl^-, Br^-, H_2S, CH_3S^-, SCN^-, CN^-, PH_3, CO, CH_3^-, H^-, C_2H_4) is exchanged for another water molecule. In further text entering and leaving water molecules will be designated as E and L, respectively (the entering ligand is supposed to be the water ligand which is more distant from the central Pt(II) atom in the transition state structure than the leaving ligand (of course the same assumption is valid for the reactant region). However in most TS—T structures the difference between the two Pt—OH_2 bond lengths is small or negligible). This experimental arrangement enables us to use principle of microscopic reversibility and also the symmetry in the preparatory stage of optimizations. However the final structures are optimized with no symmetry restrictions. Although such reactions do not have a practical importance, differences in the strength of the trans- effect of selected ligands can be evaluated and compared.

The starting reactant square- planar complexes *trans*-$Pt[(NH_3)_2(H_2O)T]^{n+}$ will be designated as R–T structures while pentacoordinated transition states and/or intermediates *trans*-$Pt[(NH_3)_2T(H_2O)_2]^{n+}$ will be designated as TS—T and INT—T, respectively.

The reaction mechanism suggests the formation of a supermolecular complex R–T$\cdots H_2O$ in the first stage. Then reaction proceeds via one TS-T transition state structure or via INT-T intermediate structure surrounded by two transition states (see Scheme 1 and Fig. 1). The activation barriers are calculated as the energy difference between TS—T and R–T$\cdots H_2O$ structures (the same approach was used with success in a number of studies (refs. 6, 9, 17, 18). Although it was shown recently by Lau and Deubel (ref. 14) that agreement of activation energies with

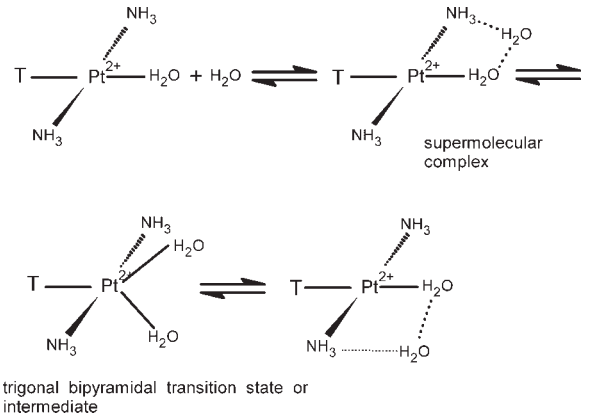

Scheme 1. Proposed reaction mechanism of substitution reactions.

experiment in the cited studies is due to large cancellation of errors, this approach is fully acceptable in our case since we are interested only in the relative (not absolute) activation energies of the reactions of the same class).

Energy Decomposition Analysis of Pt—H_2O Bond

Additional single-point calculations on the optimized structures were conducted using the Amsterdam Density Functional 2001.01 package (ADF)[33] to calculate fragment energy decompositions according to the extended transition state theory.[34] In these calculations, a triple-ζ STO basis set is utilized, with one set of polarization functions as provided in the ADF, together with the BLYP functional.[29a,c] Relativistic effects on Pt are included using the "zero order regular approximation" (ZORA).[35]

The fragment calculations available in ADF provide a decomposition of the binding energies in a chemically meaningful manner.[33] Reactant structures were considered to consist of $Pt[(NH_3)_2T]$ and H_2O fragments. The TS structures were considered to be divided into the two fragments in a number a ways: (1) $Pt[(NH_3)_2T]$ and L water ligand when E water ligand is neglected; (2) $Pt[(NH_3)_2T]$ and E water ligand when L water ligand is neglected (this analysis is done only when Pt—E and Pt—L bond lengths differ significantly); (3) $Pt[(NH_3)_2T]$ and both L and E water ligands being considered as one fragment; (4) $Pt[(NH_3)_2TL]$ and E water ligand. This enables us to make a comparison of interaction energies of E and L ligands with $Pt[(NH_3)_2T]$ fragment. The $Pt[(NH_3)_2TL]$—E decomposition gives additional information about the possible stabilization of the pentacoordinated transition states or intermediate structures.

Note that interaction energy ΔE_{int} corresponds to the bond energy of the fragments with geometries as found in original molecule. Thus the fragments are not at their equilibrium geometry resulting in higher bond energies comparing with that of true overall bond energy (the energy difference is usually called the deformation (or preparation) energy and it is the energy needed to deform the equilibrium geometries of the separate fragments to that found in the adduct structure. In case of energy decomposition analysis of R–T structures, the deformation energy of the two fragments ranges between −1.7 (R—NO_2) and −0.4 kcal/mol (R—H)—see Table 1S in the Supplementary material). The interaction energy can be further decomposed into three terms:

$$\Delta E_{int} = \Delta E_{Pauli} + \Delta E_{el-st.} + \Delta E_{orb-int}$$

The term ΔE_{Pauli} comprises the destabilizing interactions between occupied orbitals in accord with the Pauli principle. The second term $\Delta E_{el\text{-}st}$ corresponds to the classical electrostatic interaction between the charge distributions of the two fragments. These two terms can be summed to form the so called nonorbital interaction energy $\Delta E_{non\text{-}orb}$. Finally, the orbital interaction $\Delta E_{orb\text{-}int}$ accounts for charge-transfer and polarization interactions.

The R–T Complexes

Structural Features and Trans-Influence

Although the R–T structures were optimized without any constraints of symmetry they are planar. Geometrical parameters of the square planar R–T complexes are shown in the Table 1. H_2O ligand is in the trans position with respect to the T ligand. According to the decreasing Pt—OH_2 bond lengths we can order the ligands by the decreasing trans influence:

$$\begin{aligned} CH_3^- > H^- > CH_3S^- > CN^- > NO_2^- > Br^- > C_2H_4 \\ > OH^- \sim PH_3 > Cl^- \sim SCN^- > F^- > H_2S \\ > CO > NH_3 > H_2O \end{aligned}$$

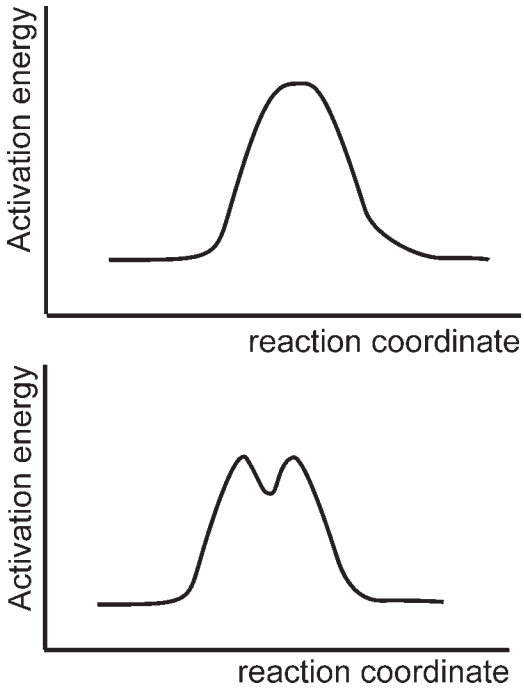

Figure 1. Possible energy profiles of substitution reactions.

Table 1. B3LYP/BSI and B3LYP/BSII Distances (in Å) in R–T Structures.

	Pt—H_2O		Pt—T		Pt—NH_3			
T/basis set	BSI	BSII	BSI	BSII	BSI	BSII	BSI	BSII
H_2O	2.066	2.065	2.066	2.065	2.087	2.086	2.087	2.086
F	2.140	2.129	1.904	1.922	2.064	2.074	2.073	2.066
OH	2.190	2.180	1.946	1.952	2.066	2.068	2.073	2.074
NH_3	2.109	2.108	2.053	2.053	2.094	2.092	2.085	2.087
SCN	2.179	2.171	1.955	1.958	2.087	2.085	2.070	2.071
Cl	2.180	2.181	2.288	2.266	2.081	2.078	2.066	2.069
Br	2.203	2.202	2.408	2.409	2.082	2.079	2.067	2.069
H_2S	2.136	2.143	2.339	2.313	2.083	2.085	2.094	2.094
NO_2	2.219	2.208	1.998	2.000	2.092	2.089	2.081	2.081
CN	2.224	2.215	1.915	1.919	2.085	2.083	2.071	2.074
PH_3	2.189	2.196	2.275	2.260	2.091	2.090	2.087	2.091
SCH_3	2.281	2.292	2.308	2.290	2.081	2.079	2.070	2.072
CO	2.125	2.122	1.876	1.881	2.099	2.097	2.091	2.093
H	2.319	2.334	1.527	1.530	2.079	2.076	2.067	2.069
CH_3	2.335	2.351	2.029	2.028	2.068	2.070	2.084	2.081
C_2H_4	2.197	2.195	2.084	2.070	2.082	2.084	2.091	2.089

The Pt—OH_2 bond trans to CH_3^- (i.e. to the ligand with the strongest trans influence) is almost by 0.3 Å longer than the Pt—OH_2 bond trans to H_2O (i.e. to the ligand with the weakest trans influence). Pt— NH_3 bond lengths are influenced significantly less by the nature of the T ligand (which is in the cis-position) ranging from 2.069 ($T{=}F^-$) to 2.095 Å (T=CO). We have not found any correlation between Pt—OH_2 and Pt— NH_3 bond lengths.

Almost the same order of ligands has been achieved after reoptimizations using substantially improved B3LYP/BSII level (see Table 1). C_2H_4, OH^-, PH_3, Cl^- ligands, i.e. ligands in the middle of the row, are mutually interchanged giving slightly modified order $PH_3 \sim C_2H_4 > Cl^- \sim OH^-$. The same is the case for F^- and H_2S ligands, trans- influence of the H_2S ligand is stronger than of the F^- ligand on B3LYP/BSII level. However these changes are subtle and give us the evidence that B3LYP/BSI method offers fairly reliable geometries.

Electronic Properties and σ-Donation

Molecular orbitals of cisplatin and related square planar Pt(II) complexes have been analyzed in a number of previous studies.[5a,7,10,27,36] Supposing that the ligands lie on the *x*,*y* axis then according to the classical ligand field theory, the $5d_{x^2-y^2}$ atomic orbital (AO) becomes LUMO of the Pt(II) fragment due to its largest repulsion with σ-donating electron pairs of ligands. The stability of the complex arises from the bonding interaction of the vacant $5d_{x^2-y^2}$ orbital of the metal with the HOMO of the ligands' fragment which is the linear combination of p_x and p_y orbitals. Since it is two-electron/two-orbital interaction, the antibonding combination of these orbitals becomes the LUMO of the complex. As electrons are donated from the filled ligand orbital to the vacant metal orbital, this kind of interaction is called σ-donation (a simplified picture for one ligand orbital is shown in Fig. 2a). It decreases the total (positive) NBO charge of the Pt(II) atom by an increase of electron density in the *xy* plane. According to the classical explanation, trans effect causes electrostatic destabilization of the ligand in the trans position and it is observable experimentally as Pt—H_2O bond length elongation (see above).

The character of the remaining 5d orbitals of the Pt(II) atom becomes nonbonding. According to the classical ligand field theory these filled nonbonding orbitals provide a repulsive interaction with the entering ligand.

NBO analysis shows that occupancies of $5d_{xy}$, $5d_{yz}$, and $5d_{z^2}$ orbitals are almost the same for different R-T structures with

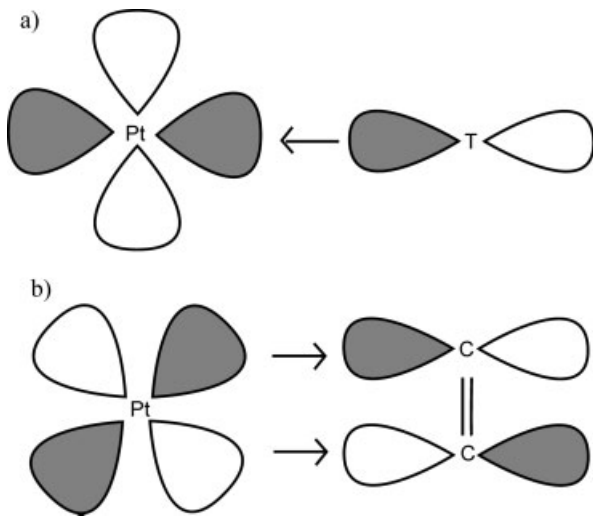

Figure 2. (a) σ-donation from the filled ligand p_x orbital to vacant metal $5d_{x^2-y^2}$ orbital. (b) π-back-donation from the filled metal d_{xz} orbital to the antibonding linear combination of carbons' p_x orbitals in C_2H_4.

Table 2. Total NBO Charges Q and AO Occupancies on Pt(II) Atom in R–T Structures.[a]

T	Q	$5d_{x^2-y^2}$	$5d_{xz}$	$5d_{xy}$	$5d_{yz}$	$5d_{z^2}$	6s
H_2O	0.845	0.815	1.989	1.970	1.987	1.855	0.517
F	0.828	0.819	1.989	1.980	1.983	1.822	0.551
OH	0.737	0.895	1.986	1.979	1.982	1.822	0.574
NH_3	0.763	0.865	1.987	1.979	1.986	1.855	0.546
SCN	0.721	0.924	1.972	1.969	1.984	1.846	0.560
Cl	0.634	0.948	1.991	1.981	1.984	1.860	0.572
Br	0.581	0.981	1.992	1.982	1.984	1.866	0.582
H_2S	0.644	0.965	1.974	1.970	1.986	1.879	0.565
NO_2	0.653	0.970	1.937	1.979	1.985	1.847	0.611
CN	0.595	1.031	1.952	1.948	1.985	1.864	0.614
PH_3	0.550	1.048	1.963	1.958	1.986	1.886	0.594
SCH_3	0.481	1.070	1.979	1.980	1.982	1.857	0.627
CO	0.726	1.013	1.884	1.894	1.989	1.887	0.598
H	0.359	1.132	1.995	1.979	1.981	1.855	0.686
CH_3	0.495	1.088	1.985	1.973	1.982	1.840	0.626
C_2H_4	0.794	1.022	1.811	1.970	1.986	1.900	0.504

[a]AO's are ordered by their importance for the trans effect strengths, not by their relative energies.

mean values of 1.968 ± 0.021, 1.984 ± 0.002, and 1.859 ± 0.021, respectively (see Table 2). On the other hand the occupancies of $5d_{x^2-y^2}$ differ substantially ranging between 0.815 (R—H_2O) and 1.132 (R—H). The $5d_{x^2-y^2}$ orbital is sd^1 hybridized with 6s orbital. Occupancy of 6s orbital increases linearly with that of $5d_{x^2-y^2}$ orbital with exception of R—C_2H_4. Figure 3 shows that the dependence of Pt—H_2O distances on $5d_{x^2-y^2}$ and 6s occupancies is linear in agreement with the theory of trans influence (see also a linear dependence of Pt—Cl bond lengths on the total platinum charge in trans-[PtClX(dms)$_2$] complexes[37] (dms = dimethylsulfide)).

The deviation of the value for R—CO complex is caused by a partial hybridization of the $5d_{x^2-y^2}$ orbital with $5d_{xy}$ orbital.

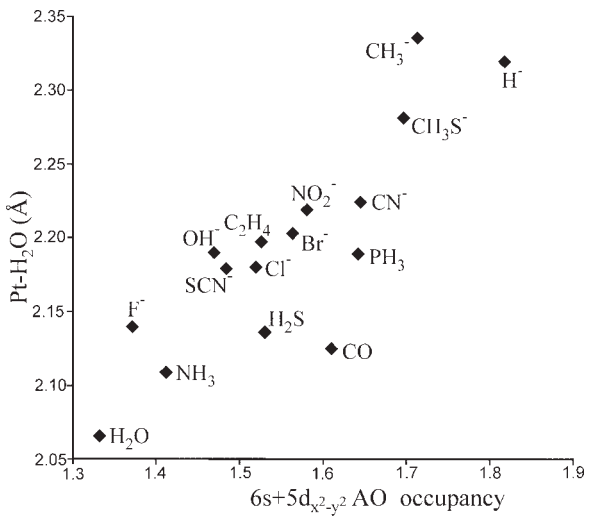

Figure 3. Dependence of Pt—H_2O distance on the occupancy of 6s and $5d_{x^2-y^2}$ AOs in R–T structures.

The latter has unusually low occupancy of 1.884. The same situation can be also seen to a smaller extent in all R-T complexes and it may be caused by the fact that the ligand-Pt-ligand angles differ from the ideal value of 90° therefore the ligands do not lay exactly on the *x*,*y* axis.

Summing up occupancy numbers of the 6s, $5d_{xy}$, and $5d_{x^2-y^2}$ AOs the following sequence of trans ligands can be constructed what may be used as a measure of the trans influence strength:

$$H^- > CH_3^- \sim CH_3S^- > PH_3 \sim CN^- > NO_2^- \sim Br^- > CO \sim Cl^- \sim H_2S \sim C_2H_4 > SCN^- \sim OH^- > NH_3 > F^- > H_2O$$

Figure 4 shows that the relationship between the occupancies of 6s, $5d_{xy}$, $5d_{x^2-y^2}$ AOs and the total H_2O ligand charge is inverse proportional. The total H_2O ligand charge reflects the amount of the charge transferred by σ-donation from H_2O ligand to the $5d_{x^2-y^2}$ orbital. Thus one would expect the above relationship should be proportional. The inverse proportional relationship between the two amounts of charges means that σ-donation ability of H_2O ligand is given by the population of the $5d_{x^2-y^2}$ orbital. The higher is the occupancy of the $5d_{x^2-y^2}$ AO the lower amount of charge can be donated by H_2O ligand to this orbital and the weaker (and longer- compare Figs. 3 and 4) is the Pt—H_2O dative bond.

Therefore we can conclude that trans influence can be understood basically as a competition between the ligands in the trans direction for the ability to donate their electron density to the $5d_{x^2-y^2}$ AO.

Further evidence for this assumption provides NBO analysis of cis- and trans- isomers of Pt[$(NH_3)_2(H)_2$]. The trans- isomer shows only a slight increase of $5d_{x^2-y^2}$ orbital occupancy with respect to R—H structure. On the other hand in the cis- isomer there is a substantial increase of $5d_{x^2-y^2}$ orbital occupancy with respect to both the trans- isomer and R—H structure (see Table 3 and Table 2).

According to our results, a classical opinion[27] that σ-donation increases electrostatic and Pauli repulsion between electrons in the metal $5d_{x^2-y^2}$ AO and electron pairs in the H_2O trans ligand

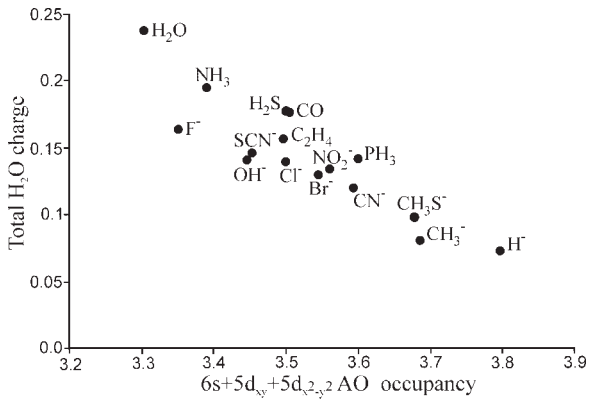

Figure 4. Dependence of total NBO charge of H_2O ligand on the AO occupancy of 6s, $5d_{xy}$ and $5d_{x^2-y^2}$ orbitals in R–T structures.

Table 3. Total NBO Charges Q and AO Occupancies on Pt(II) Atom in cis/trans-$[Pt(NH_3)_2X_2]$ Structures.

cis/trans	X	Q	$5d_{x^2-y^2}$	$5d_{xz}$	$5d_{xy}$	$5d_{yz}$	$5d_{z^2}$	6s
Trans	H	0.288	1.169	1.976	1.977	1.996	1.868	0.704
Cis	H	0.017	1.333	1.991	1.983	1.991	1.872	0.793
Trans	C_2H_4	0.704	1.072	1.813	1.983	1.987	1.908	0.514
Cis	C_2H_4	0.731	1.094	1.862	1.982	1.862	1.938	0.513

should be modified. Besides the electrostatic term also the orbital-interaction term of increases proportionally to the σ-donation. Mutual dependence of these two terms is shown in Figure 6 below. It means that relative strengths of Pt—H_2O bonds in all R-T structures studied can be also described by differences in orbital interaction energies (see below an energy decomposition analysis for more details).

π-Back-Donation

Ligands such as CO and C_2H_4 stabilize the complex also by the π-back-donation. It is interaction of the filled $5d_{xz}$ orbital (supposing the trans ligand lies on the *x* axis) with empty $\pi(p_x)$ orbitals of the ligand. Thus π-back-donation increases the total positive charge of the Pt(II) atom by a decrease of electron density in the *xz* plane. It facilitates a nucleophilic attack in the *xz* plane and stabilizes corresponding pentacoordinated transition state.

The occupancies of $5d_{xz}$ orbital are equal to almost 2.0 for most of the R-T structures (1.989 ± 0.003 for T=H_2O, NH_3, OH^-, F^-, Cl^-, Br^-, CH_3^-, H^-). Very slight lowering of the electron population of $5d_{xz}$ orbital ($\delta(d_{xz})$) was observed for R—CH_3S (1.979), R—H_2S (1.974), R—SCN (1.972) and R—PH_3 (1.963), i.e, for atoms with low-lying 3d vacant orbitals. More pronounce decrease of $\delta(d_{xz})$ occurs for R—CN (1.952) and R—NO_2 (1.937) ligands with "improperly" oriented π-system, and the most apparent reduction of $\delta(d_{xz})$ is visible for the R—CO (1.884) and especially for R—C_2H_4 (1.813). Since the *xz* plane is the plane where ligand exchange takes place the lowering of the $5d_{xz}$ orbital population enables σ-donation from filled orbitals of E and L ligands to the antibonding Pt—C orbitals. These antibonding orbitals can be characterized as linear combinations of 6s, $5d_{x^2-y^2}$ and $5d_{xz}$ platinum orbitals, however character of $5d_{xz}$ AO prevails (expansion coefficient 0.7 in case of INT—C_2H_4). The electron-repulsion decrease of the entering and leaving ligands with the orbitals of central Pt(II) atom plays slightly more significant role than in R-T structures but $\Delta E_{\text{non-orb}}$ still comprises not more than 25% of ΔE_{int} (see bellow).

Only for C_2H_4 ligand the lowering of $5d_{xz}$ orbital population is sufficient to enable the formation of the pentacoordinated intermediate minimum structure. For other trans ligands the pentacoordinated structures exist only as true transition states in case that both E and L ligands are water molecules. If E and L are e.g., OH^- ligands, minimum pentacoordinated structure was optimized also for CO ligand. The OH^- ligand forms much stronger dative bond with Pt(II) atom than the H_2O ligand as can be seen from a comparison of second order NBO energies (E^2) for LP(1)O → σ^*(Pt—C) electron donations (101.6 kcal/mol vs. 26.8 kcal/mol).

A comparison of NBO charges of cis- and trans- isomers of $Pt[(NH_3)_2(C_2H_4)_2]^{2+}$ shows that a higher positive partial charge on the platinum atom is in the cis isomer[38] since two orbitals ($5d_{xz}$ and $5d_{yz}$) are involved in π-back-donation. Only one ($5d_{xz}$) orbital is available for the two π-back-donating ligands in the trans isomer (see Table 3).

Energy Decomposition Analysis of Pt[$(NH_3)_2$T] . . . H_2O Interaction

The results are summarized in the Table 1S in the Supplementary Material. Values of ΔE_{int} for $Pt[(NH_3)_2T]\cdots H_2O$ interaction are dependent mainly on the total charge of the complex. The +2 charged systems (i.e. systems with a neutral T ligand) offer generally much lower values of ΔE_{int} than the +1 charged systems. Considering the systems with the same charge, ΔE_{int} is linearly correlated with Pt—H_2O intermolecular distances (see Fig. 5a and also refs. 13 and 39). It suggests simple electrostatic nature of the Pt—H_2O bond. However in water solvent environment (ε_r =

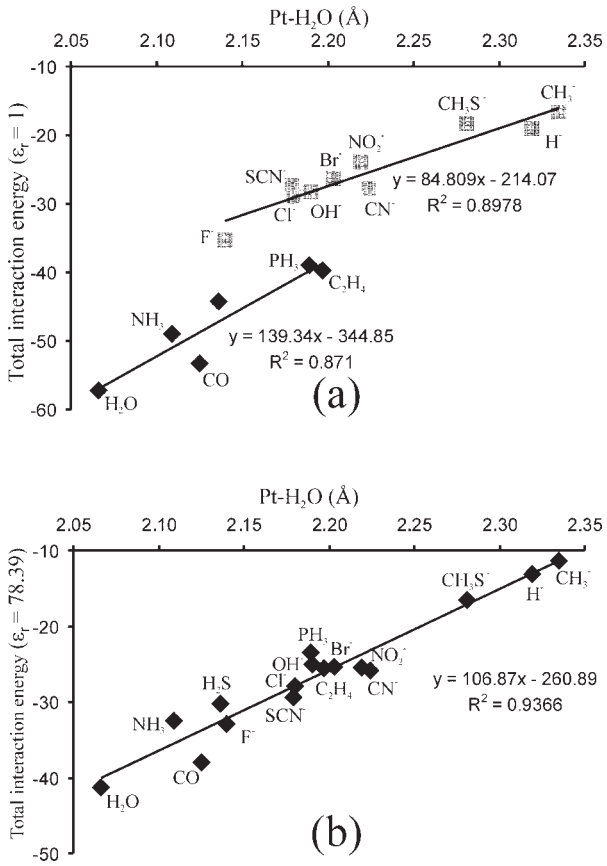

Figure 5. Total interaction ΔE_{int} and $\Delta E_{\text{int}}(w)$ energies dependence on Pt—H_2O distances in R–T structures in (a) vacuum and (b) water environment. Note that $\Delta E_{\text{int}}(w)$ energies are corrected by the deformation energies of the fragments. They are not lower than −1.7 kcal/mol (see Table 1S in the Supplementary Material) not having an important influence on the results (energies in kcal/mol).

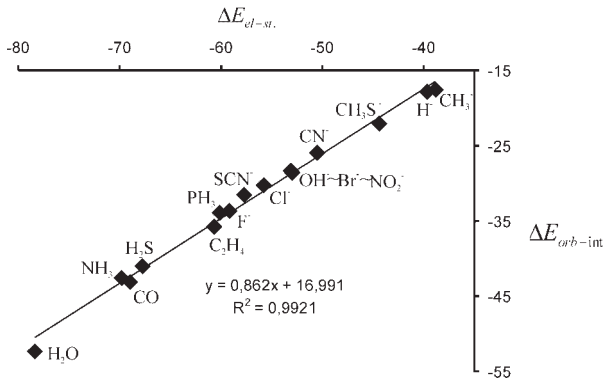

Figure 6. A mutual dependence of $\Delta E_{\text{el-st}}$ and $\Delta E_{\text{orb-int}}$ terms for $Pt[(NH_3)_2T] \cdots H_2O$ decomposition in R-T structures (in kcal/mol).

78.39) the total interaction energy $\Delta E_{\text{int}}(w)$ dependence on Pt—H_2O distance becomes linear (Fig. 5b). It is well known that long range electrostatic effects are essentially eliminated by the solvent and the dependence is then dominated by the density distribution changes (polarization and charge transfer contributions) that should not be markedly influenced by the solvent.[40]

ΔE_{int} is calculated as the sum of ΔE_{Pauli}, $\Delta E_{\text{el-st}}$, and $\Delta E_{\text{orb-int}}$ terms [Eq. (1)]. To compensate the repulsive ΔE_{Pauli} term, the $\Delta E_{\text{el-st}}$ term is usually used to form the so-called nonorbital interactions. In this case nonorbital interactions contribute only up to 20% to the total interaction energy ΔE_{int}. However in many other studies (see e.g. ref. 41 and references cited therein) instead of the $\Delta E_{\text{el-st}}$ term, $\Delta E_{\text{orb-int}}$ is used to compensate ΔE_{Pauli} term. Since the $\Delta E_{\text{orb-int}}$ term is linearly correlated with the $\Delta E_{\text{el-st}}$ term (see Fig. 6), these two ways are equivalent for R–T structures (interestingly when we have studied the dependence of the fragment energy decomposition terms on the Pt—H_2O distance for the points along the IRC pathway, for +2 charged complexes ΔE_{Pauli} was well compensated by $\Delta E_{\text{el-st.}}$ in the reactant region while in the TS region it was compensated by $\Delta E_{\text{orb-int}}$ (Figs. 1Sa) and 1Sb) in the Supplementary material). For +1 charged complexes ΔE_{Pauli} was compensated by $\Delta E_{\text{el-st}}$ on the whole reaction coordinate and ΔE_{int} follows well the $\Delta E_{\text{orb-int}}$ (Fig. 1Sc) in the Supplementary material). $\Delta E_{\text{orb-int}}$ includes a polarization term and a charge transfer component that are, indeed, closely related with the electrostatics. Figure 6 shows that for the considered R-T structures the dependence is almost exactly linear.

The covalent/ionic ratio, expressed by the ratio $\Delta E_{\text{orb-int}}/\Delta E_{\text{el-st}}$, does not differ significantly for R-T structures being 0.45 for R—H and R—CH_3, 0.54 ± 0.02 for the other +1 charged complexes and 0.61 ± 0.03 for the +2 charged complexes. Note that energy decomposition analysis is performed in the gas phase, in solution the $\Delta E_{\text{orb-int}}$ term can be expected to be the main contributor to the ΔE_{int} (w) energy (see above).

Structures Relevant for the Course of Substitution Reactions and Energetics

In the previous sections we have seen how electronic properties of R-T structures influence the mechanism of the substitution reactions. In this section let us describe the mechanism of the reaction pathways together with the relevant structures and the energetics.

The Associative Mechanism: The Trigonal Bipyramidal (TBP) INT—C_2H_4 Intermediate Structure

From the range of ligands studied, only the C_2H_4 ligand was able to stabilize both E and L water ligands in the pentacoordinated INT—C_2H_4 intermediate structure. This structure has the C_S symmetry and it is a true minimum on the potential energy surface. A similar structure was found by partial optimization in the previous study of Lin and Hall[27] but it could not be recognized as a minimum since it is a true transition state on the HF level[27] (see also ref. 42). Electron correlation effects are responsible for the stabilization of this intermediate structure as it has been proven also by the optimization on the MP2/BSI level.

Note that TBP structures of general formula [M(N—N)(olefin)XY] (M = metal; N—N = bidentate N—donor ligand; X, Y = monodentate ligands) are well experimentally described complexes.[42,43]

In the INT—C_2H_4 intermediate the E—Pt—L angle has the value of 74.0° and Pt, E, L, C_2H_4 lie in the plane which is perpendicular to the NH_3—Pt bonds. Pt—E and Pt—L bond lengths are equal to 2.39 Å, i.e. Pt—H_2O bond is elongated by 0.19 Å with respect to the R—C_2H_4 structure.

Structure and geometrical parameters of the transition state TS—C_2H_4 connecting INT—C_2H_4 intermediate with the square planar reactant R—$C_2H_4 \cdots H_2O$ are shown on the Figure 7 and in the Table 4. The Pt—E and Pt—L distances are 2.268 and 2.734 Å, respectively.

The Dissociative Interchange (I_d) Mechanism: The T-Shaped $Pt[(NH_3)_2T(H_2O)_2]^+$ ($T=H^-$, CH_3^-) Transition State Structures

Structure of transition states for ligands with the strongest trans influence, i.e. for H^- and CH_3^-, differ substantially from the other transition state structures.

H^- and CH_3^- ligands have the strongest σ-donation ability and no π-back-donation ability. It results in high populations of $5d_{x^2-y^2}$ and $5d_{xz}$ orbitals that destabilize the Pt—L bond in both the reactant and transition states structures. The substitution in the trans position proceeds clearly by a dissociative interchange (I_d) mechanism via transition state of the T-shape. Unlike the other transition states TS—H and TS—CH_3 structures are planar with E and L ligands in the plane of the complex. It is enabled by very long Pt—E and Pt—L distances being 3.075 and 3.294 Å, respectively, in TS—H; 3.684 and 3.785 Å, respectively, in TS—CH_3 (see Table 4). Pt—L and Pt—E distances are already too long to cause any interactions with filled d- orbitals on the platinum atom and they are comparable with Pt-ligand distances reported for the ligands in the first solvation shell of cisplatin-like complexes.[44,45] The position of E and L ligands in the plane of the complex is more advantageous than in the perpendicular plane since it offers ligand stabilization by the H—bond formation with NH_3 ligands. The weaker is the Pt—L (or Pt—E) interaction the stronger is the H—bonding with NH_3 ligand. In case of TS—CH_3 both E and L ligands are involved in the

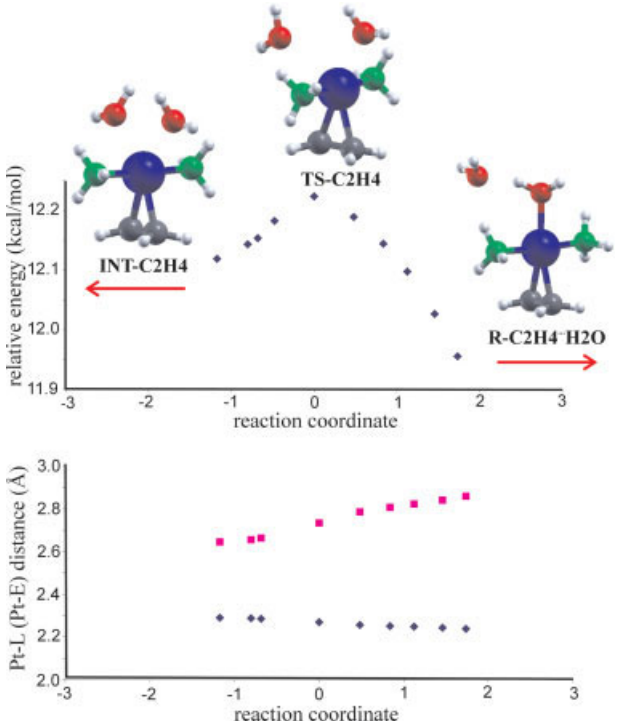

Figure 7. The IRC profile of the substitution reaction of R—C_2H_4 structure. Only a few points could be found on both directions. Their relative B3LYP/BSI energies (the upper graph) are given with respect to R—C_2H_4···H_2O structure (which has the relative energy 0.0 kcal/mol). INT—C_2H_4 structure has relative energy 11.15 kcal/mol. The direction of the INT—C_2H_4 and R—C_2H_4···H_2O structures are indicated by arrows. On the graph below Pt—E and Pt—L distances are shown.

Table 4. B3LYP/BSI Geometries of TS—T and INT—C_2H_4 Structures (Distances in Å, O—Pt—O Angles in Degrees).

T	Pt—L	Pt—E	Pt—T	Pt—NH_3		O—Pt—O
H_2O	2.408	2.426	2.110	2.070	2.084	67.2
F	2.561	2.562	1.921	2.065	2.065	60.9
OH	2.689	2.688	1.953	2.062	2.075	59.5
NH_3	2.470	2.476	2.063	2.082	2.083	66.1
SCN	2.570	2.583	1.965	2.078	2.073	62.3
Cl	2.566	2.566	2.297	2.068	2.068	63.5
Br	2.581	2.581	2.416	2.069	2.069	63.7
H_2S	2.446	2.450	2.316	2.081	2.082	68.8
NO_2	2.564	2.564	1.987	2.084	2.084	62.6
CN	2.581	2.581	1.904	2.076	2.076	63.8
CN[a]	2.610	2.610	1.906	2.075	2.075	64.1
PH_3	2.483	2.484	2.246	2.086	2.082	68.9
SCH_3	2.826	2.880	2.299	2.064	2.081	57,1
CO	2.396	2.396	1.853	2.089	2.089	68.5
CO[a]	2.407	2.407	1.856	2.089	2.089	69.5
H	3.075	3.294	1.151	2.075	2.060	53.5
CH_3	3.684	3.785	2.023	2.069	2.074	79.1
CH_3[a]	3.488	4.191	2.025	2.069	2.072	81.3
C_2H_4	2.268	2.734	2.031	2.079	2.084	76.3
INT—C_2H_4	2.39	2.393	2.005	2.082	2.082	74.0

[a]B3LYP/BSII geometries.

H—bonding towards to NH_3 groups. It results in the fairly large E—Pt—L angle of 79.1°. In case of TS—H only E is H—bonded with the NH_3 group. E is also involved in the H—bond with L ligand. It results in the lowest E—Pt—L angle of 53.5°. L is the H—bond acceptor group while E is the H—bond donor group.

Since Pt—E and Pt—L distances are not the same, E and L ligands are not fully equivalent in the TS—H and TS—CH_3 structures. As a result IRC profile is not symmetric for reverse and forward directions as both E and L ligands keep their H—bonding pattern as found in the transition state structure (see Fig. 8). However both directions lead to the same R–T···H_2O structure with oxygen atom of water involved in two H—bonds. The other H—bond pattern is not stable (structure on the reverse (negative) direction side of reaction coordinate in the Fig. 8) and rearranges to the structure R—H···H_2O upon optimization.

The Associative Interchange (I_a) Mechanism: The TBP Pt[$(NH_3)_2T(H_2O)_2$] Transition State Structures

For all the trans directors other than H^-, CH_3^-, and C_2H_4, the substitution has to overcome one TS-T transition state (T=H_2O, NH_3,

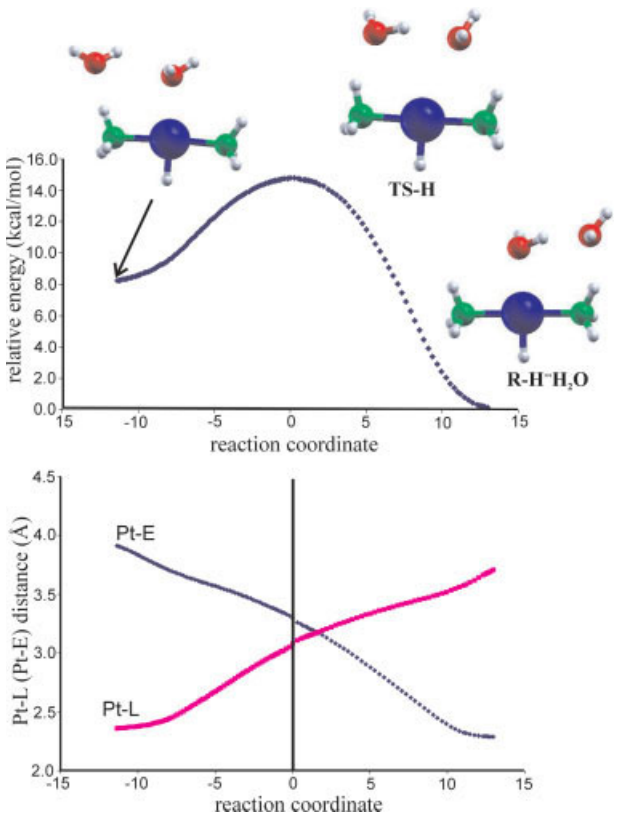

Figure 8. The IRC profile of the substitution reaction of R—H structure. B3LYP/BSI energy (the upper graph) is given with respect to R—H···H_2O structure (which has the relative energy 0.0 kcal/mol). The structure on the reverse side rearranges to R—H···H_2O structure upon optimization. On the graph below Pt-E and Pt-L distances are shown.

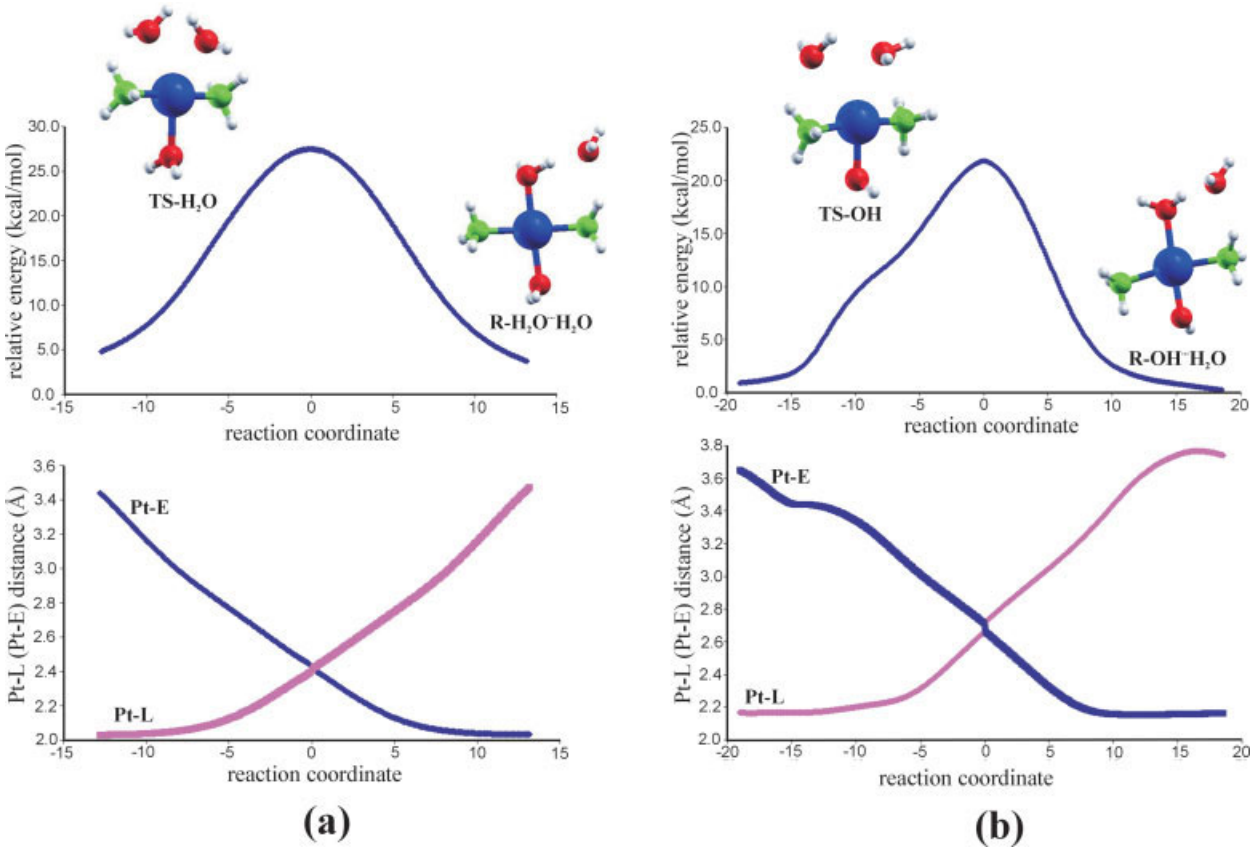

Figure 9. The IRC profiles of the substitution reactions of (a) R—H_2O and (b) R—OH structures. B3LYP/BSI energies (the upper graphs) are given with respect to R—$H_2O\cdots H_2O$ and R—$OH\cdots H_2O$ structures (what have relative energies 0.0 kcal/mol), respectively. On the graphs below Pt—E and Pt—L distances are shown. Note a steep change of these distances in the region of the TS—OH transition state.

OH^-, F^-, Cl^-, Br^-, H_2S, SCN^-, CN^-, PH_3, CH_3S^-, CO) what have the TBP structure with substantially elongated bonds towards to E and L ligands. Similar structures have already been optimized several times for cisplatin and its derivatives.[6,15,17,20,46] The elongation of Pt—L bond in TS—T structures with respect to R-T structures ranges between 0.271 (CO) and 0.545 Å (CH_3S^-) with a mean value of 0.377 Å. The other bond lengths are almost unaffected comparing to the corresponding R-T complexes. The Pt—L and Pt—E bond lengths are very similar in most of the structures (see Table 4). Thus E and L ligands can be considered to be fully equivalent in the transition state structures. The reaction can be described by an associative interchange (I_a) mechanism and a typical reaction profile is shown on the Figure 9a.

Regardless the structural similarity of the TS geometries, the calculated differences in activation barriers correspond to a ratio of reaction rates of up to seven orders of magnitude.

In the TS—OH structure E and L ligands interact by an H—bond with each other. The formation of the H—bond disturbs the symmetry of the forward reaction with respect to the reverse one as it is shown by IRC calculation (see Fig. 9b). However it has no practical importance for the general mechanism of the substitution. The H—bond formation is the reason of a fairly low E-Pt-L angle of 59.5° and of a relatively higher stabilization of E in the pentacoordinated transition state according to energy decomposition analysis.

The E ligand is rather distorted from the equatorial T—Pt—L plane in TS—CH_3S structure forming a nonlinear H—bond with NH_3 ligand (N—H···O distance of 2.018 Å and angle of 128.2°). The E ligand is also involved in additional H—bonding with L ligand leading to a fairly small E-Pt-L angle of 57.1°. The Pt-L and Pt-E bonds are rather long, more than 2.8 Å (compare with the TS structure in Fig. 1 in ref. 24). Similar geometrical features are found in TS—T ($T=H^-$, CH_3^-) structures, however in TS—CH_3S structure the H—bonds of E ligand are much weaker and Pt-L interaction is still strong enough to keep the L ligand in the equatorial plane of the TBP structure. Therefore for CH_3S ligand as the trans director, the ligand exchange proceeds by I_a rather than I_d mechanism.

The reaction mechanism may also depend on the nature of the leaving and entering ligands. For CO ligand as the trans director we have shown that strong nucleophiles (e.g. OH^- ligands as E and L) are able to stabilize minimum pentacoordinated TBP intermediate (see above) and reaction proceeds via associative mechanism.

Table 5. Relative Energies, Zero Point Energies, Enthalpy, Entropy and Solvation Corrections; and Free Energies (at 298 K) of the TS—T and INT—C_2H_4 Structures with Respect to Corresponding R—T···H_2O Structures for Ligand Exchange Reactions.

	ΔE(DFT)[a]	ΔE_{ZPE}[b]	ΔE_{TRV}[b]	$-T\Delta S$[b]	ΔE_{solv} − CPCM[c]	$\Delta G^{\ddagger}$ -DFT/CPCM
TS—H_2O	26.10	−1.67	0.46	0.70	−1.57	22.63
TS—F	24.81	−1.93	0.47	1.15	0.07	22.27
TS—OH	21.33	−1.60	0.21	0.23	1.37	21.07
TS—NH_3	24.41	−1.89	0.52	1.17	−1.64	20.23
TS—SCN	21.48	−2.02	0.50	0.80	0.68	19.83
TS—Cl	20.57	−1.98	0.50	1.02	−0.04	18.02
TS—Br	19.07	−1.92	0.46	0.71	0.06	16.96
TS—H_2S	19.25	−1.62	0.40	0.51	−1.42	16.10
TS—NO_2	17.65	−1.93	0.52	1.24	0.28	15.28
TS—CN	17.97	−2.04	0.54	1.19	−0.62	14.65
TS—PH_3	16.59	−1.63	0.42	0.50	−1.44	13.44
TS—SCH_3	14.64	−1.50	1.28	3.69	2.41	13.15
TS—CO	17.44	−1.28	0.31	0.25	−3.27	12.95
TS—H	12.77	−1.81	0.21	0.64	0.79	11.31
TS—CH_3	10.06	−2.02	0.65	3.38	5.43	10.74
TS—C_2H_4	11.01	−1.49	0.30	0.43	−1.15	8.24
INT—C_2H_4	10.27	−1.18	0.68	1.27	−2.76	5.74

All energies are in kcal/mol.
[a]B3LYP/ MWB-60(2fg)/6-311++G(2df,2dp)//B3LYP/6-31G* values.
[b]B3LYP/6-31G* corrections.
[c]B3LYP-CPCM/ MWB-60(2fg)/6-311++G(2df,2dp)// B3LYP/6-31G* corrections.

Activation Free Energies and the Kinetic Trans-Effect

Activation free energies $\Delta G^{\ddagger}$ are directly related with the kinetic constant of the reaction by a factor $e^{-\Delta G^{\ddagger}/RT}$. Since the trans effect is a kinetic phenomenon relative activation free energies correspond to the expected relative strengths of the trans effect. We can order the ligands according to the activation energies (see Table 5), which these ligands provoke in the trans position:

$$C_2H_4 >> CH_3^- \sim H^- > CO \sim CH_3S^- \sim PH_3 > CN^- \sim NO_2^- \sim H_2S > Br^- > Cl^- > SCN^- \sim NH_3 \sim OH^- > F^- \sim H_2O$$

The water H_2O ligand and the ethylene C_2H_4 ligand show the weakest and the strongest trans effect, respectively.

The total NBO charges on the central Pt(II) atom in the reactant structures correlate proportionally with the heights of the activation barriers (see Fig. 10). The lower is the total NBO charge on the Pt(II) atom the lower is the activation free energy. This dependence is almost linear with important exceptions of CO and C_2H_4 ligands. Their activation energies are too low with respect to their total NBO charges. It suggests that σ-donation is the prevailing effect for all the ligands except of CO and C_2H_4 ligands, which deviation reflects the extent of the π-back donation (see also a dependence of the activation free energies on the 6s, $5d_{xy}$ and $5d_{x^2-y^2}$ AOs occupancies in Fig. 2S).

Since the NBO charges correlate linearly with activation energies and simultaneously also with the Pt—H_2O trans- ligand distances in R-T structures, it is not surprising that there is a linear dependence between Pt—H_2O distances and heights of activation barriers (see Fig. 11). It is in accord with the trans influence theory and it suggests Pt—H_2O (or Pt—L) bond breaking energy is a dominant contribution to activation free energy (see also ref. 23). Again the C_2H_4 and CO ligands are exceptions where the TS structure stabilization by π-back donation plays important role.

TS Geometry: Energy Decomposition Analysis for Pt[(NH$_3$)$_2$T] and L Fragments when E Water Ligand is Neglected

Values of ΔE_{int} for the transition states are linearly correlated with ΔE_{int} energies in the reactant structures, i.e. the stronger is ΔE_{int} energy in the reactant structure the stronger it is also in

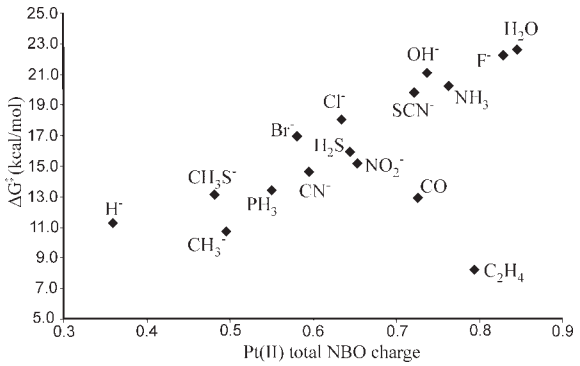

Figure 10. Activation free energy dependence on the total NBO charge of the Pt atom in R–T structures.

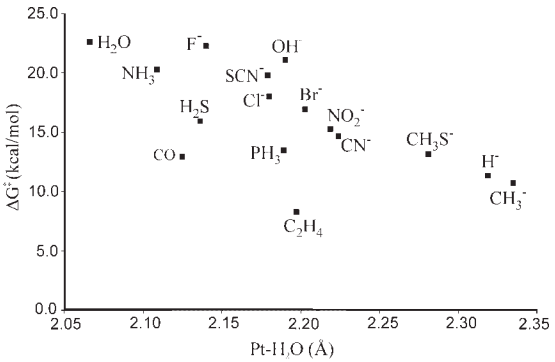

Figure 11. Dependence of activation free energies on Pt—H_2O distances in R–T structures.

the corresponding transition state (compare Tables 1S and 2S in the Supplementary Material). Absolute value of ΔE_{int} energy increases linearly with the decreasing Pt—H_2O distance with exception of CH_3 and H ligands where stabilization of L through the H—bonding with the NH_3 group is important.

Relative importance of $\Delta E_{non\text{-}orb}$ terms is higher in TS-T structures than in R-T structures. It is caused by a relatively higher decrease of the ΔE_{Pauli} term comparing to $\Delta E_{el\text{-}st}$ and $\Delta E_{orb\text{-}int}$ terms. For TS—H, $\Delta E_{non\text{-}orb}$ energy makes even 62% of ΔE_{int} energy showing a strong H—bond formation between the E water molecule and the complex but it is substantially less for the other TS—T structures.

Since L and E water ligands are equivalent in most of the TS structures, energy decomposition analysis for Pt[$(NH_3)_2$T] and both L and E water ligands being considered as one fragment gives results that are exactly in line with the above described ones (see Table 3S and Fig. 3S in the Supplementary Material).

TS Geometry: Energy Decomposition Analysis for Pt[$(NH_3)_2$TL] and E Water Ligand Fragments

As in previous cases, value of ΔE_{int} for the Pt[$(NH_3)_2$TL] $\cdots$ E interaction is dependant mainly on the charge of the complex. The +2 charged systems offers generally much lower ΔE_{int} values (see Table 4S in the Supplementary Material). The lowest ΔE_{int} values were calculated for INT—C_2H_4 and TS—CO structures suggesting the highest stabilization of the fifth ligand in the complex. ΔE_{int} values in other +2 charged systems are lower by about 20 kcal/mol.

Values of ΔE_{int} for +1 charged systems are about half of that for +2 charged systems. From +1 charged systems the lowest ΔE_{int} values offer structures with additional H—bond E ligand stabilization such as TS-OH and surprisingly also TS—H and TS—CH_3 where H—bonding can be considered as the only source of stabilization. This statement can be supported by a comparison of these results with the Pt[$(NH_3)_2$T]$\cdots$E decompositions. ΔE_{int} values for Pt[$(NH_3)_2$TL]$\cdots$E structures are increased substantially except the Pt[$(NH_3)_2$HL]$\cdots$E decomposition. Increase of ΔE_{int} values is caused by both (1) an increase of ΔE_{Pauli} repulsion term due to presence of L water molecule and (2) a decrease of $\Delta E_{orb\text{-}int}$. The $\Delta E_{el\text{-}st}$ term is almost unchanged what shows that E and L water ligands do not interact with each other. For the Pt[$(NH_3)_2$HL]$\cdots$E decomposition, an increase of $\Delta E_{el\text{-}st}$ and $\Delta E_{orb\text{-}int}$ terms fully compensates the increase in ΔE_{Pauli} repulsion term suggesting an H—bond formation between E and L water ligands.

Conclusions

In this contribution we show that reactivity of Pt(II) square planar complexes is driven by two effects: σ-donation and π-back-donation. Their importance can be quantified by the population of $5d_{x^2-y^2}$ and $5d_{xz}$ AOs, respectively (in case the ligands lie in the xy plane with trans- directing ligands on the x axis). The first effect is linearly correlated with the Pt—H_2O (leaving ligand) bond length prolongations (i.e. trans- influence, see Fig. 3). In solution the Pt—H_2O bond lengths are linearly correlated with the total interaction energies between the leaving H_2O ligand and the rest of the complex (see Fig. 5b). Nearly linear dependence was found also for dependence of activation free energies on Pt—H_2O distances (see Fig. 11) with exceptions of C_2H_4 and CO ligands. It means that the kinetic trans effect is determined by the strength of the trans influence (i.e. by σ-donation ability—see Fig. 10) except the ligands with strong π-back-donation ability such as C_2H_4 and CO that stabilize transition state structure.

Pt(II)-ligand bonds are described as typical donor- acceptor bonds, non-orbital interactions contribute only up to 20% to the total interaction energy. The σ-donation ability of the ligand is dependant on the σ-donation ability of the ligand in the trans position (but not in the cis- position). Therefore there is a competition between the ligands in the trans- position for the opportunity to donate their electron density to the central Pt(II) atom (see Fig. 4 and Table 3). Similarly two π-back-donating ligands in trans position compete with each other to some extent since the two ligands withdraw electron density from the same ($5d_{xz}$) orbital.

The influence of the trans- effect on the reaction mechanism is also shown. When a ligand with a very strong σ-donation (such as CH_3^- and H^-) is present the total electron occupation in the $5d_{x^2-y^2}$ orbital is higher. It prevents the trans-ligand to form a strong dative bond with the central Pt(II) atom by σ-donation. Only formation of a very weak Pt—H_2O bond is allowed. Substitution proceeds by a dissociative interchange (I_d) mechanism.

On the other hand ligands such as ethylene C_2H_4 and CO show only a moderate trans- effect but they lower electron occupation in the $5d_{xz}$ orbital by a π-back donation. It decreases electron density on the Pt(II) atom in the xz plane and it leads to the stabilization of the pentacoordinated transition state/intermediate and the substitution proceeds by an associative mechanism. Existence of the stable pentacoordinated intermediate structure on the potential energy surface depends on the nucleophilicity of the entering and leaving ligands. In case of CO ligand the pentacoordinated intermediate structure exists for OH^- ligands being the entering and leaving ligands but not for a weak nucleophile such as H_2O ligand. C_2H_4 ligand is able to stabilize pentacoordinated intermediate structure for both H_2O and OH^- ligands being the entering and leaving ligands.

The other ligands (T=H_2O, NH_3, OH^-, H_2S, F^-, Cl^-, Br^-, SCN^-, CN^-, PH_3, CH_3S^-) in the trans- position show weak or

moderate σ-donation and π-back-donation abilities. The substitution reactions have to overcome higher activation barriers and they proceed via one transition state of the TBP shape with substantially elongated bonds towards to leaving and entering ligands. Their mechanism corresponds to a associative interchange (I_a) mechanism.

References

1. Chernyaev, I. I. Ann Inst Platine (USSR) 1926, 4, 423.
2. (a) Fleischhacker, A. S.; Matthews, R. G. Biochemistry 2007, 46, 12382; (b) Albeniz, A. C.; Espinet, P.; Martin-Ruiz, B. Dalton Trans 2007, 33, 3710; (c) Berezin, D. B.; Toldina, O. V.; Berezin, B. D. Russ J Inorg Chem 2006, 51, 1728; (d) Chermette, H.; Rachedi, K.; Volatron, F. J Mol Struct (Theochem) 2006, 762, 109; (e) Randaccio, L.; Geremia, S.; Nardin, G.; Wuerges, J. Coord Chem Rev 2006, 250, 1332; (f) Sergienko, V. S. Crystallogr Rep 2004, 49, 907.
3. (a) Banerjea, D.; Basolo, F.; Pearson, R. G. J Am Chem Soc 1957, 79, 4055; (b) Basolo, F.; Gray, H. B.; Pearson, R. G. J Am Chem Soc 1960, 82, 4200; (c) Gosling, R.; Tobe, M. L. Inorg Chem 1983, 22, 1235; (d) Wendt, O. F.; Elding, L. I. Inorg Chem 1997, 36, 6028; (e) Wendt, O. F.; Elding, L. I. J Chem Soc Dalton Trans 1997, 4725; (f) Kuznik, N.; Wendt, O. F. J Chem Soc Dalton Trans 2002, 15, 3074; (g) Otto, S.; Elding, L. I. J Chem Soc Dalton Trans 2002, 11, 2354.
4. (a) Melnik, M.; Holloway, C. E. Coord Chem Rev 2006, 250, 2261; (b) Dedieu, A. Chem Rev 2000, 100, 543; (c) Wong, E.; Giandomenico, C. M. Chem Rev 1999, 99, 2451; (d) Fuertes, M. A.; Alonso, C.; Perez, J. M. Chem Rev 2003, 103, 645; (e) Jamieson, E. R.; Lippard, S. J. Chem Rev 1999, 99, 2467; (f) Hush, N. S.; Schamberger, J.; Bacskay, G. B. Coord Chem Rev 2005, 249, 299.
5. (a) Basch, H.; Krauss, M.; Stevens, W. J.; Cohen, D. Inorg Chem 1985, 24, 3313; (b) Carloni, P.; Andreoni, W.; Hutter, J.; Curioni, A.; Giannozzi, P.; Parrinello, M. Chem Phys Lett 1995, 234, 50; (c) Wysokinski, R.; Michalska, D. J Comput Chem 2001, 22, 901; (d) Deubel, D. V. J Am Chem Soc 2004, 126, 5999; (e) Michalska, D.; Wisokinski, R. Chem Phys Lett 2005, 403, 211.
6. Chval, Z.; Sip, M. J Mol Struct (Theochem) 2000, 532, 59.
7. Pavankumar, P. N. V.; Seetharamulu, P.; Yao, S.; Saxe, J. D.; Reddy, D. G.; Hausheer, F. H. J Comput Chem 1999, 20, 365.
8. Burda, J. V.; Leszczynski, J. Inorg Chem 2003, 42, 7162.
9. Burda, J. V.; Zeizinger, M.; Leszczynski, J. J Comput Chem 2005, 26, 907.
10. Burda, J. V.; Zeizinger, M.; Sponer, J.; Leszczynski, J. J Chem Phys 2000, 113, 2224.
11. Zeizinger, M.; Burda, J. V.; Leszczynski, J. Phys Chem Chem Phys 2004, 6, 3585.
12. Lopes, J. F.; Menezes, V. S. D.; Duarte, H. A.; Rocha, W. R.; De Almeida, W. B.; Dos Santos, H. F. J Phys Chem B 2006, 110, 12047.
13. Deubel, D. V. J Am Chem Soc 2002, 124, 5834.
14. Lau, J. K.-C.; Deubel, D. V. J Chem Theory Comput 2006, 2, 103.
15. Chval, Z.; Sip, M. Collect Czech Chem Commun 2003, 68, 1105.
16. Costa, L. A. S.; Hambley, T. W.; Rocha, W. R.; De Almeida, W. B.; Dos Santos, H. F. Int J Quantum Chem 2006, 106, 2129.
17. Costa, L. A. S.; Rocha, W. R.; De Almeida, W. B.; Dos Santos, H. F. J Chem Phys 2003, 118, 10584.
18. Raber, J.; Zhu, C. B.; Eriksson, L. A. J Phys Chem B 2005, 109, 11006.
19. Zhang, Y.; Guo, Z. J.; You, X. Z. J Am Chem Soc 2001, 123, 9378.
20. Baik, M. H.; Friesner, R. A.; Lippard, S. J. J Am Chem Soc 2003, 125, 14082.
21. Deubel, D. V. J Am Chem Soc 2006, 128, 1654.
22. Mantri, Y.; Lippard, S. J.; Baik, M. H. J Am Chem Soc 2007, 129, 5023.
23. Cooper, J.; Ziegler, T. Inorg Chem 2002, 41, 6614.
24. Lau, J. K.-C.; Deubel, D. V. Chem Eur J 2005, 11, 2849.
25. Zhu, J.; Lin, Z. Y.; Marder, T. B. Inorg Chem 2005, 44, 9384.
26. Braunschweig, H.; Brenner, P.; Müller, A.; Radacki, K.; Rais, D.; Uttinger, K. Chem Eur J 2007, 13, 7171.
27. Lin, Z. Y.; Hall, M. B. Inorg Chem 1991, 30, 646.
28. Gaussian 03, Revision C. 02,Frisch, M. J.; Trucks, G. W.; Schlegel, H. B.; Scuseria, G. E.; Robb, M. A.; Cheeseman, J. R.; Montgomery, J. A., Jr.; Vreven, T.; Kudin, K. N.; Burant, J. C.; Millam, J. M.; Iyengar, S. S.; Tomasi, J.; Barone, V.; Mennucci, B.; Cossi, M.; Scalmani, G.; Rega, N.; Petersson, G. A.; Nakatsuji, H.; Hada, M.; Ehara, M.; Toyota, K.; Fukuda, R.; Hasegawa, J.; Ishida, M.; Nakajima, T.; Honda, Y.; Kitao, O.; Nakai, H.; Klene, M.; Li, X.; Knox, J. E.; Hratchian, H. P.; Cross, J. B.; Adamo, C.; Jaramillo, J.; Gomperts, R.; Stratmann, R. E.; Yazyev, O.; Austin, A. J.; Cammi, R.; Pomelli, C.; Ochterski, J. W.; Ayala, P. Y.; Morokuma, K.; Voth, G. A.; Salvador, P.; Dannenberg, J. J.; Zakrzewski, V. G.; Dapprich, S.; Daniels, A. D.; Strain, M. C.; Farkas, O.; Malick, D. K.; Rabuck, A. D.; Raghavachari, K.; Foresman, J. B.; Ortiz, J. V.; Cui, Q.; Baboul, A. G.; Clifford, S.; Cioslowski, J.; Stefanov, B. B.; Liu, G.; Liashenko, A.; Piskorz, P.; Komaromi, I.; Martin, R. L.; Fox, D. J.; Keith, T.; Al-Laham, M. A.; Peng, C. Y.; Nanayakkara, A.; Challacombe, M.; Gill, P. M. W.; Johnson, B.; Chen, W.; Wong, M. W.; Gonzalez, C.; Pople, J. A. Gaussian, Inc.: Pittsburgh PA, 2003.
29. (a) Becke, A. D. Phys Rev A 1988, 38, 3098; (b) Vosko, S. H.; Wilk, L.; Nusair, M. Can J Phys 1980, 58, 1200; (c) Lee, C. T.; Yang, W. T.; Parr, R. G. Phys Rev B 1988, 37, 785; (d) Becke, A. D. J Chem Phys 1993, 98, 5648.
30. Andrae, D.; Haussermann, U.; Dolg, M.; Stoll, H.; Preuss, H. Theor Chim Acta 1990, 77, 123.
31. Reed, A. E.; Weinhold, F. J Chem Phys 1983, 78, 4066.
32. Weinhold, F.; Landis, C. R. Chem Ed Res Pract (CERP; special "Structural Concepts" issue) 2001, 2, 91.
33. Velde, G. T.; Bickelhaupt, F. M.; Baerends, E. J.; Guerra, C. F.; Van Gisbergen, S. J. A.; Snijders, J. G.; Ziegler, T. J Comput Chem 2001, 22, 931.
34. (a) Ziegler, T.; Rauk, A. Theor Chim Acta 1977, 46, 1; (b) Ziegler, T.; Rauk, A. Inorg Chem 1979, 18, 1558; (c) Ziegler, T.; Rauk, A. Inorg Chem 1979, 18, 1755.
35. (a) van Lenthe, E.; Baerends, E. J.; Snijders, J. G. J Chem Phys 1993, 99, 4597; (b) van Lenthe, E.; van Leeuwen, R.; Baerends, E. J.; Snijders, J. G. Int J Quantum Chem 1996, 57, 281.
36. Baik, M. H.; Friesner, R. A.; Lippard, S. J. J Am Chem Soc 2002, 124, 4495.
37. Kapoor, P. N.; Kakkar, R. J Mol Struct (Theochem) 2004, 679, 149.
38. Hofmann, A.; Jaganyi, D.; Munro, O. Q.; Liehr, G.; van Eldik, R. Inorg Chem 2003, 42, 1688.
39. Mrázek, J.; Burda, J. V. J Chem Phys 2006, 125, 194518.
40. Burda, J. V.; Sponer, J.; Hrabakova, J.; Zeizinger, M.; Leszczynski, J. J Phys Chem B 2003, 170, 5349.
41. Frenking, G.; Frohlich, N. Chem Rev 2000, 100, 717.
42. Albano, V. G.; Natile, G.; Panunzi, A. Coord Chem Rev 1994, 133, 67.
43. Albano, V. G.; Monari, M.; Orabona, I.; Ruffo, F.; Vitagliano, A. Inorg Chim Acta 1997, 265, 35.
44. Berges, J.; Caillet, J.; Langlet, J.; Kozelka, J. Chem Phys Lett 2001, 344, 573.
45. Naidoo, K. J.; Klatt, G.; Koch, K. R.; Robinson, D. J. Inorg Chem 2002, 41, 1845.
46. Burda, J. V.; Zeizinger, M.; Leszczynski, J. J Chem Phys 2004, 120, 1253.